ISAS - INTERNATIONAL SCHOOL
FOR ADVANCED STUDIES

Electron Localization
and
Pauli Principle

Thesis submitted for the degree of

"Magister Philosophiæ"

CANDIDATE

Lorenzo De Santis

SUPERVISOR

Prof. Raffaele Resta

October 1997

SISSA - SCUOLA
INTERNAZIONALE
SUPERIORE
STUDI AVANZATI

TRIESTE
Via Beirut 2-4

TRIESTE

SISSA ISAS
SCUOLA INTERNAZIONALE SUPERIORE DI STUDI AVANZATI
INTERNATIONAL SCHOOL FOR ADVANCED STUDIES

Electron Localization and Pauli Principle

Thesis submitted for the degree of

"Magister Philosophiæ"

CANDIDATE

Lorenzo De Santis

SUPERVISOR

Prof. Lorenzo De Santis

October 1997

Table of Contents

1 Density functionals

1.1 Introduction

The celebrated basic tenet of density–functional theory (DFT) [1] states that an exact description of a many electron system is in principle possible in terms of a single scalar field, namely the electron density $n(\mathbf{x})$. The N-electron wavefunction and the associated Schrödinger equation contain instead redundant information; in extendend systems, the N-electron wavefunction does not even have a well defined thermodynamic limit.

DFT is based on an exact theorem due to Hohenberg and Kohn (HK) [1] , but its enormous success resides in approximate schemes that—when implemented with first–principles ingredients—have proved over the years their very accurate predictive power for many physical properties, in many different materials.

Historically the first attempt of such a theory is the Thomas–Fermi approximation [2]. The electrons are treated semiclassically, and their distribution in phase space is obtained from the idea that the electrons are locally distributed as an homogeneous electron gas. From this assumption, it is easy to extract an energy functional of the charge density only, whose variation determines the ground state energy and the ground state charge

density. The Thomas–Fermi approximation is a simple intuitive approach, providing an approximate description of the average density and a plausible estimate of the ground state energy. However, the approximation is at best a qualitative one, and basically does not allow quantitative predictions.

The modern approximations to DFT—whose basic paradigm is the local–density approximation (LDA)—are qualitatively different from the Thomas–Fermi approximation, in that they are *not* density–only functionals. In fact, one invariably needs to evaluate, as an intermediate step, a set of one–particle orbitals: the Kohn–Sham (KS) orbitals [3]. The energy of the N-electron system is then expressed as a function of them, notably in the kinetic–energy term. In the quest for simplified and/or more efficient DFT schemes, possibly achieving the so–called "order N" scaling, an orbital–free descriptions of the many–electron system is desirable.

The present work is an analysis of the electron distribution in various real systems, where very different kinds of bonds are present. Our study is *a-posteriori*, and is indeed based on an orbital description à la KS: actual calculations are performed within DFT–LDA, using norm–conserving pseudopotentials. We analyze the electron distributions using some novel and very powerful tools, in order to gather information about the features that any simplified but realistic DFT scheme should reproduce.

1.2 The N-representability problem

The milestone HK theorem has shown how a theory in terms of density was far more fundamental than previously imaginated, establishing a one-to-one mapping between the ground

state electron density $n(\mathbf{x})$ and the external potential $v(\mathbf{x})$ for a system of N interacting fermions with a nondegenerate ground state. Other important hypotheses are that the sistem is finite, and that no magnetic field is present.

Since $n(\mathbf{x})$ univocally determines N and $v(\mathbf{x})$, and hence all ground–state properties, HK have also defined an energy functional $E[n]$, which reaches its minimum when $n(\mathbf{x})$ is equal to the exact ground–state density of the interacting electronic system.

Some difficulties were left aside both on practical and theoretical grounds: the former is about the actual determination of the energy functional, since all the correlation effects remain hidden in the exchange and correlation potential. The latter concerns some mathematical subtleties not considered in the original HK work, and goes under the name of the v-representability problem [4]. However, disregarding this formal detail seems not to have serious practical consequences in most physical circumstances.

A still open question, directly connected to the determination of an optimal energy functional, is instead the N-representability problem, which concerns the reconstruction of the antisymmetric many body wavefunction generating a given density. Even if one can easily construct an entire family of antysimmetric N-electron wave functions corresponding to a given reasonable density [5], the energy associated to this trial wavefunctions is far from being the true ground state energy, even in the simple case of non interacting electrons. This happens because fixing the density is not sufficient to restrict the Hilbert space to an "acceptable" subset of many body wavefunctions and a very special attention must be paid to the kinetic energy. In fact, at least in the simple case of independent electrons, the only term appearing in the Hamiltonian not directly dependent on the charge density is the

kinetic one.

A direct and simple tool to analize the spatial variations of the kinetic energy density is the electron localization function (ELF), introduced by Becke and Edgecombe [6] in the context of the electron localization, but reinterpreted by Savin and coworkers [7] as the natural method to univocally define the local behaviour of kinetic energy density with respect to an homogeneous reference system. Therefore, once we have calculated the ELF within a certain framework (such as DFT–LDA in our case), we can use this information to naturally check or even to construct new energy functionals.

1.3 A novel solution to the N-representabilty problem

The N-representability problem was formally solved by Harriman [5] in one dimension. For any given density, the Harriman construction provides an explicit independent–electron (alias single–determinant) wavefunction for the N-electron system. One can thus explicitly write the electronic energy (including the kinetic one) as a functional of the density only. But the Harriman construction restricts the variational freedom of the wavefunction. Therefore a minimization of this functional provides in general an energy which is higher than the ground–state energy. The reasons for this will be clear below, when we discuss our own solution of the three–dimensional N-representabilty problem.

The one–dimensional Harriman construction has been generalized to the three–dimensional case by Zumbach and Maschke [8]). Here we present a more general and more elegant three–dimensional construction, based on an adaptive metric in coordinate space. Our general finding encompasses the Zumbach–Maschke result as a very particular case, which is (dis-

turbingly) even little symmetrical in the Cartesian coordinates. Furthermore, our metric approach emphasizes the different contributions to the local kinetic energy density, and makes contact with the usual ELF definition [7] discussed in a subsequent Chapter.

For a system of independent electrons in a closed–shell configuration the wavefunction is a single determinant: knowledge of the one–particle reduced density matrix is equivalent to a complete knowledge of the wavefunction. The spin–integrated matrix γ is twice a projector, which indeed projects over the (doubly occupied) one–particle orbitals.

We start considering a generic homogeneous system of N non-interacting fermions in a box of volume Ω, obeying periodic boundary conditions: we use the variable ξ for the space coordinates of this homogeneous system. The orbitals are obviously plane waves; any single determinant of plane waves has constant density (*i.e.* is homogeneous). The minimum–energy determinant is obtained by occupying the orbitals below the Fermi energy: this yields the spin–integrated density matrix:

$$\gamma_0(\boldsymbol{\xi},\boldsymbol{\xi}') = \frac{2}{\Omega}\sum_{l=1}^{N/2} e^{i\mathbf{k}_l(\boldsymbol{\xi}-\boldsymbol{\xi}')}. \tag{1.1}$$

This matrix is idempotent, that is:

$$\int d\boldsymbol{\xi}''\gamma_0(\boldsymbol{\xi},\boldsymbol{\xi}'')\gamma_0(\boldsymbol{\xi}'',\boldsymbol{\xi}') = 2\gamma_0(\boldsymbol{\xi},\boldsymbol{\xi}') \tag{1.2}$$

and its diagonal yelds the uniform charge density n_0:

$$n(\boldsymbol{\xi}) = \gamma_0(\boldsymbol{\xi},\boldsymbol{\xi}) = \frac{N}{\Omega} = n_0. \tag{1.3}$$

The idea now is to introduce a coordinate mapping, in the same spirit as in the Gygi [9] adaptive curvilinear coordinate calculations:

$$\boldsymbol{\xi} \longrightarrow \mathbf{x}(\boldsymbol{\xi}). \tag{1.4}$$

The metric tensor is usually expressed as

$$g_{ij} = \frac{\partial x^k}{\partial \xi^i}\frac{\partial x^k}{\partial \xi^j} \tag{1.5}$$

(summation over repeated indices is used) and plane waves in curvilinear coordinates are transformed to

$$\frac{1}{\sqrt{\Omega}} e^{i\mathbf{k}\boldsymbol{\xi}} \longrightarrow \chi_{\mathbf{k}}(\mathbf{x}) = \frac{1}{\sqrt{\Omega}} g^{-\frac{1}{4}}(\mathbf{x}) e^{i\mathbf{k}\boldsymbol{\xi}(\mathbf{x})} \tag{1.6}$$

where $g = \det g_{ij}$, $|\frac{\partial x}{\partial \xi}| = g^{-\frac{1}{2}}$ is the Jacobian of the transformation $\mathbf{x} \to \boldsymbol{\xi}(\mathbf{x})$ and $\mathbf{k}$ is a reciprocal lattice vector. The density matrix in the new coordinates is given by

$$\gamma(\mathbf{x}, \mathbf{x}') = \gamma_0(\boldsymbol{\xi}(\mathbf{x}), \boldsymbol{\xi}(\mathbf{x}')) = \frac{2}{\Omega} g^{-\frac{1}{4}}(\mathbf{x}) g^{-\frac{1}{4}}(\mathbf{x}') \sum_{l=1}^{N/2} e^{i\mathbf{k}_l[\boldsymbol{\xi}(\mathbf{x}) - \boldsymbol{\xi}(\mathbf{x}')]} \tag{1.7}$$

and the transformed density is given again by the diagonal as

$$n(\mathbf{x}) = n_0 g^{-\frac{1}{2}}(\mathbf{x}). \tag{1.8}$$

Therefore the system is no longer homogeneous in the transformed coordinates, but the density matrix remains idempotent by construction. The number of the electrons in the box is conserved, therefore the average density of the nonhomogeneous system is n_0, the same as for the homogeneous one.

We are now ready to attribute physical content to the above mathemathics. Suppose that the density of a given electronic system $n(\mathbf{x})$ is known. Then we may look for a coordinate transformation $\boldsymbol{\xi} \longrightarrow \mathbf{x}(\boldsymbol{\xi})$ which maps the uniform density into the given density: a necessary and sufficient condition is given by Eq. (1.8). The solution is nonunique, since several different maps share the same Jacobian $g^{-\frac{1}{2}}$: we will argue below about an optimal choice. The Zumbach–Maschke result can be regarded as a very special choice fullfilling

Eq. (1.8). The one–dimensional analogue of our construction is unique, and coincides with Harriman's one. For any given metric which fullfills Eq. (1.8), we may recast the density matrix, Eq. (1.7), as:

$$\gamma(\mathbf{x},\mathbf{x}') = \frac{2}{N} n^{\frac{1}{2}}(\mathbf{x}) n^{\frac{1}{2}}(\mathbf{x}') \sum_{l=1}^{N/2} e^{i\mathbf{k}_l[\boldsymbol{\xi}(\mathbf{x})-\boldsymbol{\xi}(\mathbf{x}')]}. \tag{1.9}$$

This density matrix is idempotent by construction, and provides therefore an explicit solution of the N-representabilty problem. For any given density, we construct—in an elegant and general way—an idempotent density matrix, which in turn is in one–to–one correspondence to a single–determinant wavefunction.

1.4 A density–only functional

Since we now have an explicit one–particle reduced density matrix, we may express the energy of the noninteracting–electron system in terms of the density and of the metric tensor. The Hamiltonian is:

$$H = -\frac{\hbar^2}{2m}\nabla^2 + v(\mathbf{x}) \tag{1.10}$$

and the potential expectation value over the $\chi_{\mathbf{k}}$ basis is:

$$\langle \mathbf{k}|V|\mathbf{k}\rangle = \frac{1}{\Omega}\int d\boldsymbol{\xi}\; v(\mathbf{x}(\boldsymbol{\xi})) = \frac{1}{\Omega}\int d\mathbf{x}\; v(\mathbf{x}) g^{-\frac{1}{2}}(\mathbf{x}). \tag{1.11}$$

The summation over all the electrons yelds the usual result

$$\langle v\rangle = \int d\mathbf{x}\; v(\mathbf{x}) n(\mathbf{x}). \tag{1.12}$$

Following the formulas given in Ref. [9], the kinetic energy term can be partitioned into the sum of a gauge potential term and of the usual quadratic term:

$$\langle \mathbf{k}|T|\mathbf{k}\rangle = \langle \mathbf{k}|T_{gauge}|\mathbf{k}\rangle + \langle \mathbf{k}|T_{quad}|\mathbf{k}\rangle. \tag{1.13}$$

Defining the gauge potential A_i as:

$$A_i = \frac{1}{4}\frac{\partial \ln g}{\partial \xi^i}, \tag{1.14}$$

the T_{gauge} term is given by:

$$\langle \mathbf{k}|T_{gauge}|\mathbf{k}\rangle = \frac{1}{\Omega}\frac{\hbar^2}{2m}\int d\boldsymbol{\xi}\; A_i g^{ij} A_j. \tag{1.15}$$

Summing over the N occupied states, and considering (1.8), we get:

$$\langle T_{gauge}\rangle = \frac{\hbar^2}{2m}\frac{n_0}{16}\int d\mathbf{x}\; g^{-\frac{5}{2}}(\mathbf{x})|\nabla g|^2 = \frac{\hbar^2}{8m}\int d\mathbf{x}\; \frac{|\nabla n(\mathbf{x})|^2}{n(\mathbf{x})}. \tag{1.16}$$

The last expression in (1.16) shows that $\langle T_{gauge}\rangle$ can be interpreted as the ground state kinetic energy of a system of N non-interacting bosons at density $n(\mathbf{x})$; it can be easily proved [10] that it provides a rigorous lower limit for the exact kinetic energy of a fermionic system having the same density.

It follows that the remaining quadratic term is the contribution due to the Pauli principle, a natural measure of the local effectiveness of the statistical correlations on the kinetic energy density. The expectation value over the $\chi_{\mathbf{k}}$ basis is:

$$\langle \mathbf{k}|T_{quad}|\mathbf{k}\rangle \equiv \langle \mathbf{k}|T_{Pauli}|\mathbf{k}\rangle = \frac{1}{\Omega}\frac{\hbar^2}{2m}k_i k_j \int d\boldsymbol{\xi}\; g^{ij}. \tag{1.17}$$

Considering, for sake of simplicity, a cubic box and summing over all $\mathbf{k}$, we obtain:

$$\langle T_{Pauli}\rangle = \frac{E_0}{3\Omega}\int d\mathbf{x}\; g^{-\frac{1}{2}}\, tr\{g^{ij}\}, \tag{1.18}$$

where E_0 is the kinetic energy of the homogeneous system, defined as:

$$E_0 = \frac{\hbar^2}{2m}\sum_{l=1}^{N/2} k_l^2. \tag{1.19}$$

Putting all of the above results together, we get the energy as a functional of the density and of the metric as:

$$\langle E \rangle = \frac{E_0}{3\Omega} \int d\mathrm{x}\, g^{-\frac{1}{2}}\, tr\{g^{ij}\} + \frac{\hbar^2}{8m} \int d\mathrm{x}\, \frac{|\nabla n(\mathrm{x})|^2}{n(\mathrm{x})} + \int d\mathrm{x}\, v(\mathrm{x}) n(\mathrm{x}). \tag{1.20}$$

At this point, we may easily define the optimal metric as the one that, for a given $n(\mathrm{x})$, provides the minimum value of $\langle E \rangle$.

In the trivial case of free electrons, $v(\mathrm{x}) = 0$, we have a uniform density $n(\mathrm{x}) = n_0$. The metric is the identity and only the first term survives in the r.h.s. of Eq. (1.20): the Pauli energy coincides with the energy of the free fermions, and our functional provides for $\langle E \rangle$ the *exact* result.

For the nonhomogenoues case, considering the inequality

$$\frac{1}{3} tr\, g \geq (\det g)^{\frac{1}{3}} \tag{1.21}$$

we obtain for the Pauli term

$$\langle T_{Pauli} \rangle \geq \frac{E_0}{3\Omega n_0^{\frac{2}{3}}} \int d\mathrm{x}\, n^{\frac{5}{3}}(\mathrm{x}). \tag{1.22}$$

The r.h.s. of (1.22) is the characteristic Thomas–Fermi kinetic energy functional.

As a consequence we can argue that a single coordinate transformation satysfing (1.8), applied to the ground state of an homogeneous system, gives a kinetic energy equal to its lower bosonic limit plus a term always greater than the jellium limit. The only way to gauge the quality of a single–determinant wavefunction is to understand how the true kinetic energy density deviates from its bosonic lower limit. As it will be clear in a while, the ELF is exactly a measure of this deviation, and from the ELF plots reported below it is evident how in covalent or ionic systems, the kinetic energy, particularly along the bonding

direction, reaches its minimum (bosonic) value. The only systems where the kinetic energy is almost equal to its Thomas Fermi limit are the bulk metals, where the coordinate mapping (1.8) should give a good approximation to the true ground state many body wavefunction.

2 The Electron Localization Function

2.1 Definitions

As anticipated in the introduction, the ELF was proposed by Becke and Edgecombe [6] in the study of electron localization. Although this might seem a rather ill–defined problem, a precise and unambiguous definition of the electron localization it is an highly non trivial task, and provides a wealthy of relevant information about the electron distribution. In the past, several workers have attempted different practical recipes in order to define localization domains, but all of them, in one way or another, are affected by a series uncontrolled approximations.

A first attempt toward an orbital–independent description of electron localization has been made by Bader and Essen [11], with the study of the charge density Laplacian $\nabla^2 n$. They showed how the structure of the Laplacian in an atom reflects its shell structure, there being a shell of charge concentration and one of charge depletion associated with each quantum shell. This method, however, fails for heavy atomic systems [12], since Laplacian often does not reveal more than five atomic shells. Also its huge variability, ranging from

negatively infinite value at atomic nuclei to unbounded positive value elsewhere, is somewhat inconvenient for purposes of graphical representation, as depicted in the lover panels of Fig. (2.1).

Becke and Edgecombe [6] investigated a different approach to define regions of space where the electrons are "more" or "less" localized. They introduced the ELF as a measure of the probability of finding an electron in the neighborhood of another electron with the same spin. Starting from the short range behavior of the parallel–spin pair probability, they defined a new scalar function, conveniently ranging from zero to one, that uniquely identifies regions where the electrons are well localized. This new function can be defined either for independent electrons, or for correlated ones. In the independent–electron case the ELF is invariant under unitary transformations of the occupied orbitals, and is therefore function solely of the one–particle reduced density matrix. This is the case of interest to us, since as explained below we will investigate the ELF at the KS level. The ELF has always the same symmetry of the electronic charge density and naturally reveals atomic shell structure, chemical bonds and lone electron pairs. As a simple example, we report in the upper panels of Fig. (2.1) our ELF calculations for two noble gas atoms, to show how the atomic shell structure is reproduced in a remarkably clear and simple manner.

An alternative and more enlightening interpretation of the same function has been proposed by Savin and coworkers [7], who considered the *excess local kinetic* energy due to the Pauli repulsion. This is the kind of ELF we are going to investigate below for several condensed matter systems.

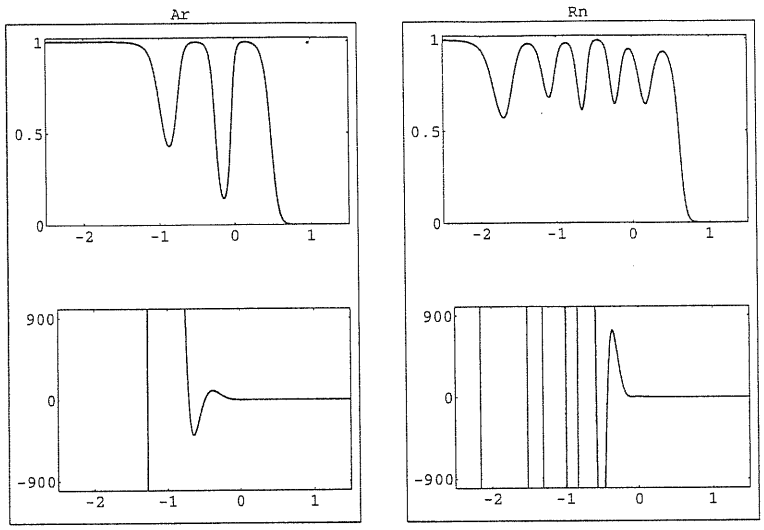

Figure 2.1: ELF (upper panels) and Laplacian in atomic units (lower panels) for Ar and Rn. The calculation are performed within the DFT (see text). Logarithmic scale along x axes.

The KS local kinetic energy density is:

$$\tau(\mathbf{x}) = -\frac{\hbar^2}{2m}\nabla_{\mathbf{x}}\nabla_{\mathbf{x}'}\gamma(\mathbf{x},\mathbf{x}')\Big|_{\mathbf{x}=\mathbf{x}'} \tag{2.1}$$

where γ is again the single particle density matrix. Indicating the ground state kinetic energy of a non-interacting system of bosons with $\tau^B(\mathbf{x})$, the explicit expression for the ELF $\mathcal{E}(\mathbf{x})$ is:

$$\mathcal{E}(\mathbf{x}) = \frac{1}{1+(D/D_h)^2}, \tag{2.2}$$

where

$$D(\mathbf{x}) = \tau(\mathbf{x}) - \tau^B(\mathbf{x}) \geq 0 \tag{2.3}$$

can be easily interpreted as an estimate of the increase of the local kinetic energy density due to the Pauli principle, and D_h is the same quantity calculated for the homogeneous electron gas at the same density.

In other words, the ELF provides a convenient measure for the local bosonic behaviour of the electron density. In the regions of space where the electrons are alone or form pairs of opposite spins ELF is close to one, because D tends to its lower limit: the Pauli principle has indeed little influence and the electrons almost behave like bosons. Notice that for any two–electron system the wavefunction is strictly bosonic, with a nodeless wavefunction in coordinate space, and $\mathcal{E}(\mathbf{x}) \equiv 1$ everywhere. On the other side, ELF tending to zero means strong Pauli repulsion due to the parallel spin electrons, with the special value ELF$= 1/2$ indicating a local jellium-like electron distribution.

2.2 Technical details

Several authors have investigated ELF in atoms and molecules, where correlated wavefunctions are available. These studies have shown that the corresponding analysis of the independent–particle ELF, based either on the Hartree–Fock approximation or on the KS orbitals in the DFT–LDA scheme, reproduces the main features in a number of different systems. Of course, the kinetic energy of the KS noninteracting electrons is different from the kinetic energy of the interacting system, but this differences does not distort significantly the ELF analysis. Because of this previous experience, and since correlated wavefunctions for solids are not easily available, our ELF studies in condensed matter are performed using the KS kinetic energy, where the KS orbitals have been obtained within DFT–LDA. The electronic charge density is written in terms of the KS orbitals, as:

$$n(\mathbf{x}) = \sum_i |\phi_i^{KS}(\mathbf{x})|^2, \tag{2.4}$$

and the same orbitals also enter in the definition of the local kinetic energy density, computed directly from (2.1) for a one-determinant wavefunction, as

$$\tau^{KS}(\mathbf{x}) = \frac{\hbar^2}{2m}\sum_i^N |\nabla\phi_i^{KS}(\mathbf{x})|^2. \tag{2.5}$$

Using the homogeneous electron gas, we get for the Pauli kinetic energy density the value

$$D_h(\mathbf{x}) = \frac{3\hbar^2}{20m}(3\pi^2)^{\frac{2}{3}}n(\mathbf{x})^{\frac{5}{3}}. \tag{2.6}$$

It is important to remark how all the ELF plots reported in this work display vanishing ELF in asymptotic regions, or where the electronic density itself approaches zero. This is a consequence of the $n^{\frac{5}{3}}$ denominator, vanishing much more strongly than the excess local kinetic energy (except the case where D it is *identically* zero, as in a two electron atom).

We use a standard plane-wave expansion for the KS orbitals, solving the self consistent KS equations for the Fourier coefficients of the orbitals. To get rid of the fast oscillations of the solution, due to the core electrons, which would require an enormous basis size to be described with acceptable resolution, we used the pseudo-potential approximation, in its usual non local, norm conserving form [13].

Neglecting the core requires some care, because ELF is defined in terms of the all-electron charge density. From the formal point of view, we can expect good results from a valence only approach when both valence and core orbitals do not have large contributions in the same region of space. Kohut and Savin [14] made and extensive study on ELF computed from the valence density *alone* (i.e. with the summation index in (2.4) and (2.5) running on the valence orbitals) and they stressed how ELF computed from the total density differs substantially from the *valence* ELF, particularly when the penultimate d orbitals tend to

penetrate the valence region and their exclusion in (2.4) summation produce a considerably enhancement of ELF value. Anyhow, in the present study, we limit ourselfs to first and second row compounds, where the pseudopotential approximation is entirely justified. Our *pseudo*-ELF, outside the core region, concides perfectly with the true all-electron ELF, the only difference being trivially the absence of core shells (i.e. there is a hole in the core region for the pseudo-charge diagrams).

2.3 Application to ionic, covalent and metallic bulk systems

ELF is a tool naturally devoted to the qualitative study of ionicity effects upon the bond character. We report in Fig. (2.2) and Fig. (2.3) our results for, respectively, a group of covalent systems and the limiting cases of a metal and a ionic compound.

For the zincblende semi-conductors in Fig. (2.2), ordered with increasing Phillips ionicity [15], we have observed effects analogous to those cited in Ref. [16] for similar structures. The effect of bond polarity is nicely revealed by the ELF, that shows mainly two features: first of all, the bond character is strictly bosonic (black regions), with a strongly directioned region between the two atoms, where the Pauli principle has little influence and the formation of a bond electron pair is allowed. Secondarily, the region of high ELF value becomes increasingly asymmetric and extended, with a clear tendency to concentrate around the more electronegative atom. In agreement with Ref. [16], we have also found a good correlation between the ratio of covalent radii and the distance of the ELF maxima from the relative nuclei.

The ionic crystal KBr, reported in Fig. (2.3), is simply the limiting case of Fig. (2.2),

with each Br atom surrounded by a nearly spherical cloud of high ELF value, corresponding to the filled valence shell. A much more interesting situation is, instead, the metallic bulk aluminum, where the black region has disappeared, leaving a wide-spread grey region corresponding to a jellium-like ELF values. This behaviour is consistent with the phenomenological free electron picture usually adopted for metals, but it is strictly in contrast with standard textbook description of the metallic bond, which could be naively thought as a particular case of the covalent one. In the metallic systems, instead, the statistical correlations due to the Pauli principle play a very special role, better understood now via this ELF plot, which shows how the electronic charge density is almost uniformly fermionic, in contrast with the strong bosonic behaviour in the covalent bonded systems.

2.4 Metallic surfaces

In this final section, we present our ELF calculation for several metallic surfaces. The Al [001] surface presents a rather surprising result, particularly compared with the bulk case considered in Fig. (2.3). In Fig. (2.4) and (2.5) we show the charge density and the ELF in two different crystalline planes of the [001] surface. As expected, far from the surface is reproduced the bulk system of Fig. (2.3), while the most intriguing feature is the thin surface layer of high ELF values, indicating a surface electron localization corresponding to a local increase in the bosonic character of charge density, otherwise well described in the bulk with a jellium approximation.

This surface effect is nicely revealed with a ELF *macroscopic average*, along the surface normal. The concept of macroscopic average is a basic one in classical electromagnetism [17]

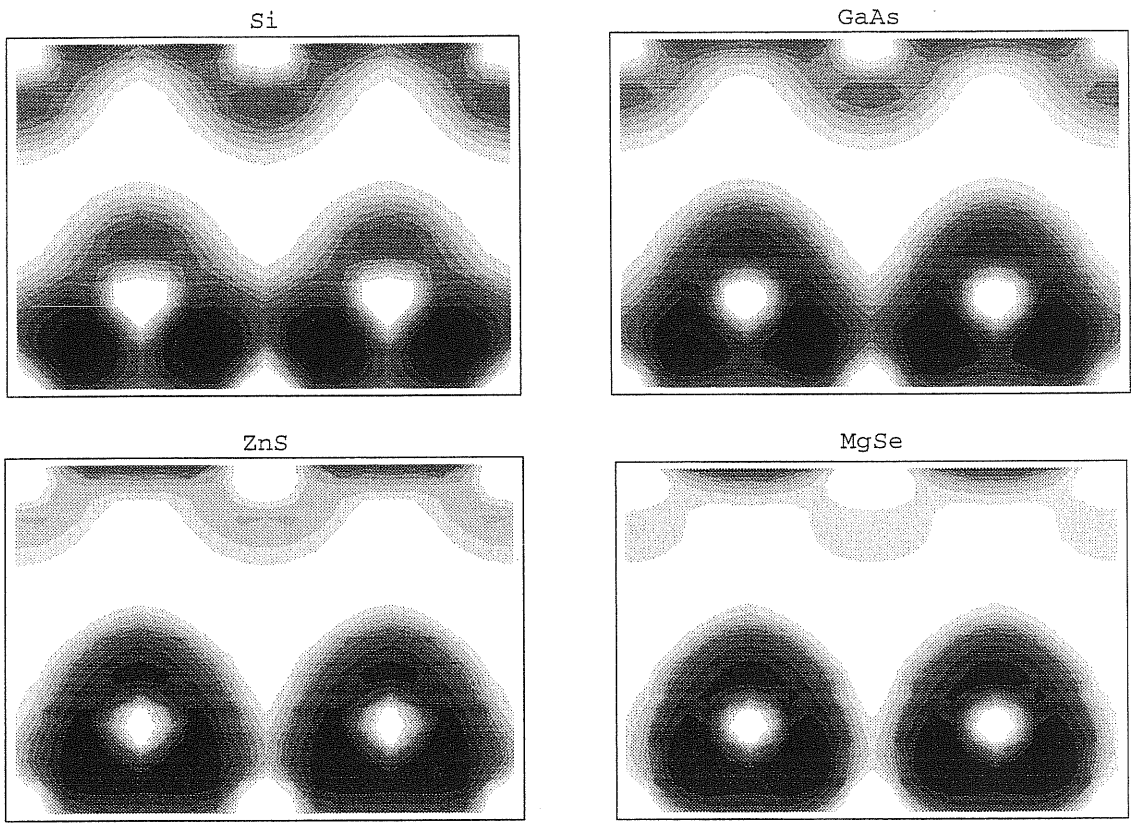

Figure 2.2: Contour plots of ELF in the [110] plane for different zinc-blend structures, with increasing bond ionicity. Dark regions correspond to large ELF values, bright to small ones.

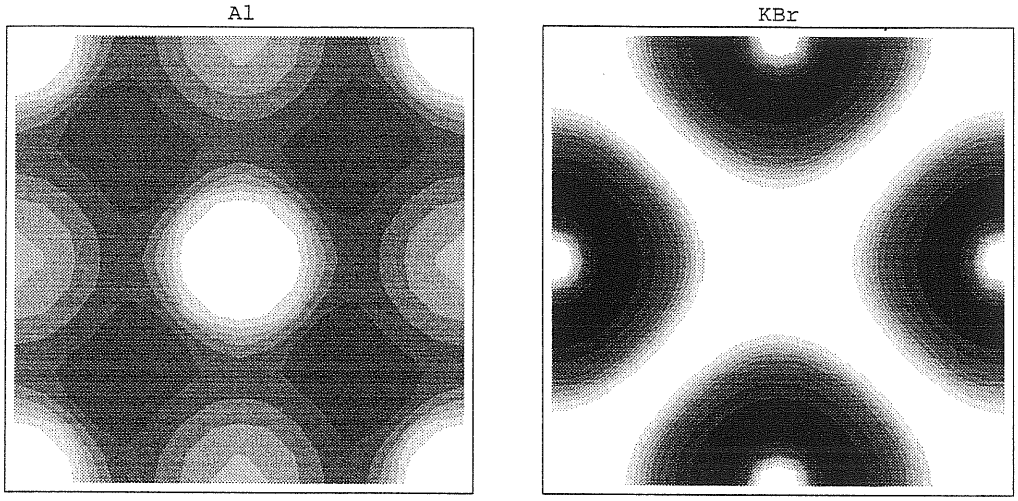

Figure 2.3: Contour plots of ELF in the [100] plane for Al and KBr. Conventions as in Fig. (2.2).

and it is the usual trick to wash out the microscopic oscillations from any lattice periodic function. In this way, any macroscopic quantity $\overline{f}$ is related to its microscopic counterpart f through a suitable convolution:

$$\overline{f}(\mathbf{x}) = \int w(\mathbf{x} - \mathbf{x}')f(\mathbf{x}')d\mathbf{x}', \tag{2.7}$$

where $w(\mathbf{x})$ is the (real) filter function, nonzero in some neighborhood of $\mathbf{x} = 0$ and normalized to unity over all the space. The use of macroscopic average has turned out to be of fundamental importance in the heterojunction problem [18], because it allowed to clarify the physics at the interfaces with no introduction of any artificial or unnecessary concept. In the present work, the macroscopic average is a natural approach to disregard the microscopic oscillations of ELF and to univocally separate the bulk from the surface behaviour.

Indicating with z the direction orthogonal to the surface and considering the system

periodicity in the (x, y) plane, the first step is to take the planar average of ELF as function of the z-coordinate alone:

$$\overline{\mathcal{E}}(z) = \frac{1}{S}\int_S \mathcal{E}(x, y, z)dxdy. \tag{2.8}$$

From the ELF plotted in Fig. (2.4) and Fig. (2.5), we obtain the planar average in Fig. (2.6). The next step is to convolute this one dimensional function with a step function, to get rid of the microscopic oscillations:

$$\overline{\overline{\mathcal{E}}}(z) = \frac{1}{a}\int_{z-\frac{a}{2}}^{z+\frac{a}{2}} \overline{\mathcal{E}}(z')dz' = \frac{1}{a}\int \Theta\left(\frac{a}{2} - |z - z'|\right)\bar{\mathcal{E}}(z')dz', \tag{2.9}$$

where a is the unit cell. The result is shown in Fig. (2.6) and it is now immediate to see how the macroscopic average allows to define, in an unambiguous way, the concept of local "charge bosonization".

We have also observed a similar effect in the [001] silicon surface. This surface is strongly reconstructed, with several different reconstructed structures. A relatively simple (2×1) reconstruction is formed by surface atoms moving together in pairs to form dimers. The driving force for the dimers formation is the elimination of a dangling bond from the surface atoms. Each atom of the unreconstructed surface (Fig. 2.7) is bonded to only two neighbours and therefore has two dangling bonds projecting out of the surface. If the atoms move together in pairs, forming a new bond between them, then one of these dangling bonds will be eliminated from each member of the pair (Fig. 2.8). We have considered therefore the unreconstructed and the (2×1) symmetric dimer surfaces, in order to better understand the connection between surface reconstruction and electronic localization.

As we should expect from classical quantum mechanics consideration, every dangling bond is associated to an isolated electron, thus corresponding to a local increase in ELF

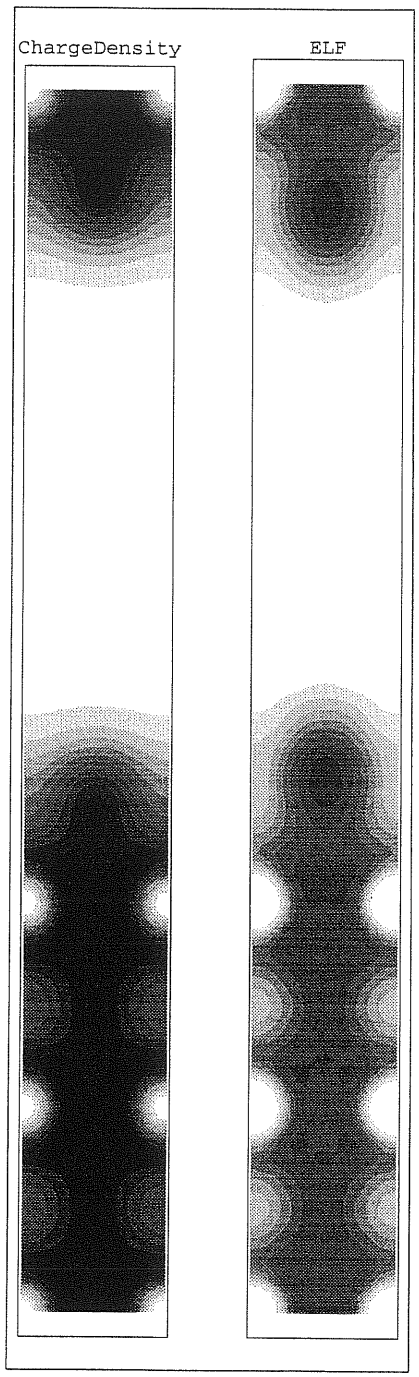

Figure 2.4: Charge density and ELF for a [001] Al slab. [001] supercell plane. Conventions as in Fig. (2.2).

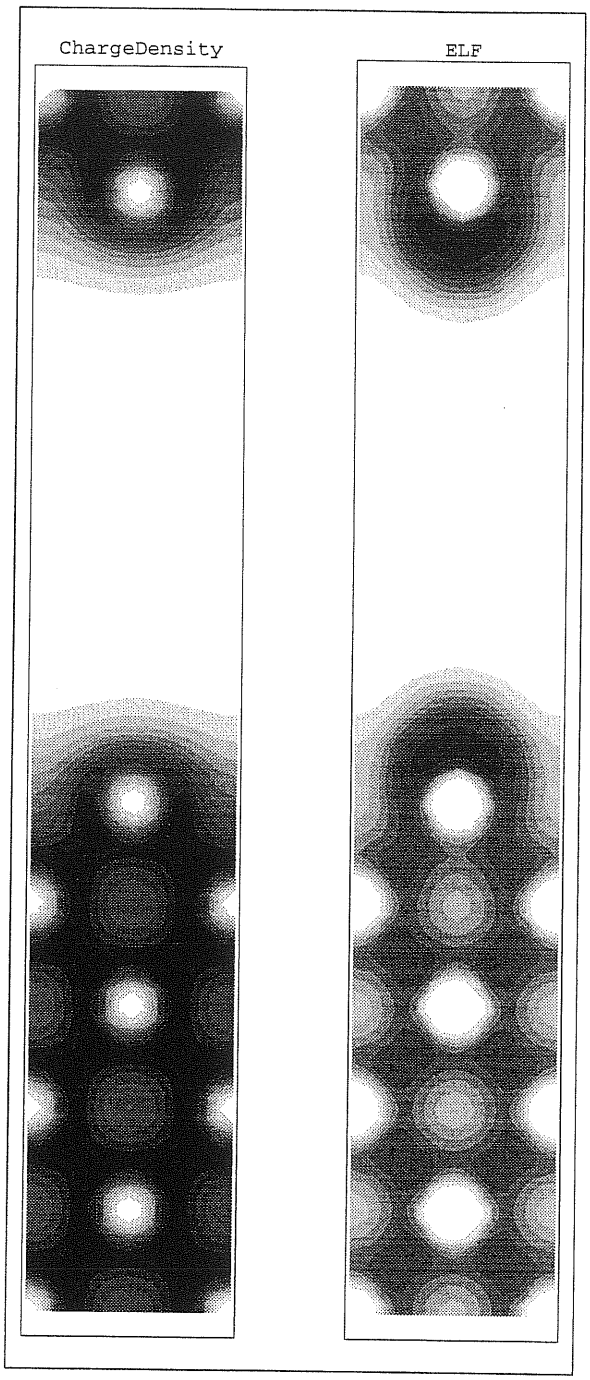

Figure 2.5: Charge density and ELF for a [001] Al slab. [110] supercell plane, corresponding with the [100] bulk plane in Fig. (2.3). Conventions as in Fig. (2.2).

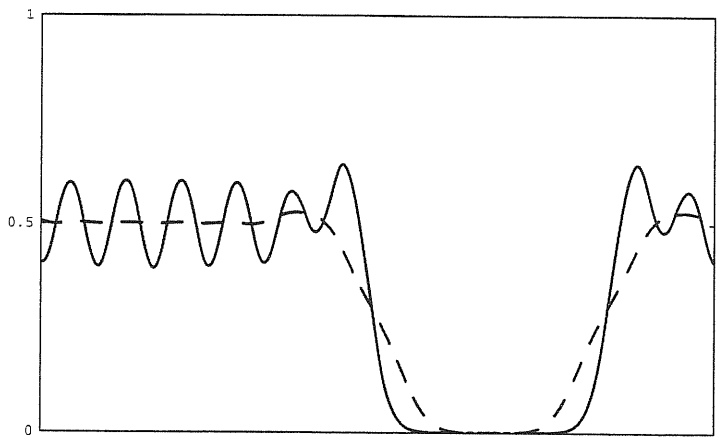

Figure 2.6: ELF for the aluminum slab. Planar average along the direction orthogonal to the surface (solid line), with superimposed the ELF macroscopically averaged (dashed line).

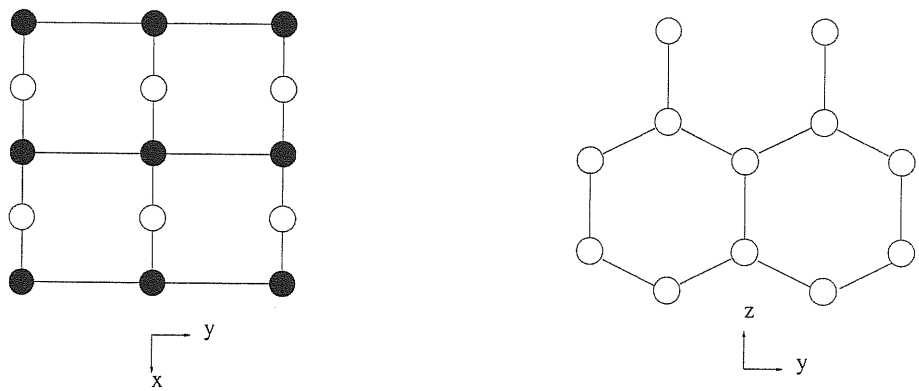

Figure 2.7: Top and lateral view of the unreconstructed [001] silicon surface. White circles in the top view represent atoms in the surface layer and black circles represent atoms in the second layer. The z direction is orthogonal to the surface plane.

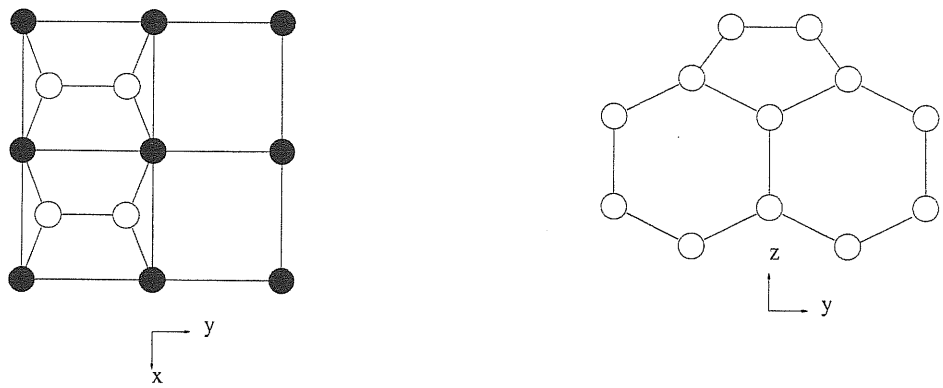

Figure 2.8: Top and lateral view of the symmetric (2 × 1) dimer reconstruction of [001] silicon surface. Convections as in Fig. (2.7).

value. In Fig. (2.9) is reported charge density and ELF in the plane containing the dangling orbitals and the two atoms participating to the dimer formation, with the two orbitals well emphasized by the ELF plot. However the most striking feature is the presence of fermionic "surface channel" between the two dangling atoms, corresponding to a delocalized charge density. This channel in the bond midpoint has a perfect circular section (Fig. 2.10), but it is actually formed by two grey-ELF strips (Fig. 2.11) arranged along the silicon surface and intersecting in the unit cell center. As it was stressed from the aluminum case, the ELF of a metallic surface tends to form bosonic regions, instead of a monotonical decay, from its average jellium value (ELF= $\frac{1}{2}$), to zero outside of the surface. Hence the presence of this wide-spread jellium system along the unrelaxed surface should be connected to the strong surface strain, due to the free dangling atoms. As soon as surface is relaxed and the dimer formation is allowed, there is a strong surface bosonization, associated with a sizeable reduction of this fermionic channel. For the symmetric dimerized (2 × 1) surface, we have reproduced the Roberts and Needs [19] calculation, with a 10 Ry basis set cut-off and 16

k-point on a Monkhorst and Pack [20] mesh for the Brillouin zone integration. We have also used directly their relaxed atomic coordinates, to reduce the atomic forces. In Fig. (2.12) we report the symmetric dimer reconstructed surface where, comparing with Fig. (2.11), it is noticeable the localization effect due to the dimerization process. The same effect is also well observed in the plane orthogonal to the surface, containing the dimer (Fig. 2.13), which has a strongly covalent bond character and is surrounded by a region of high ELF values.

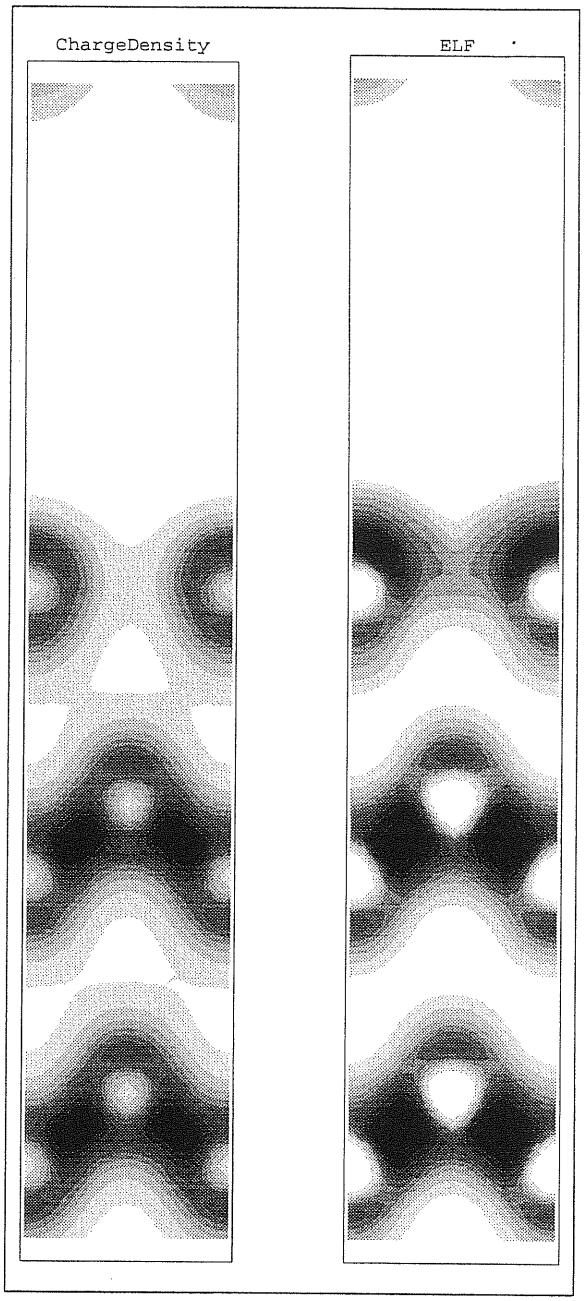

Figure 2.9: Charge density and ELF for the [001] bulk terminated silicon surface. Plane containing the two atoms participating to the dimer formation and the relative dangling orbitals, revealed by the black ELF regions.

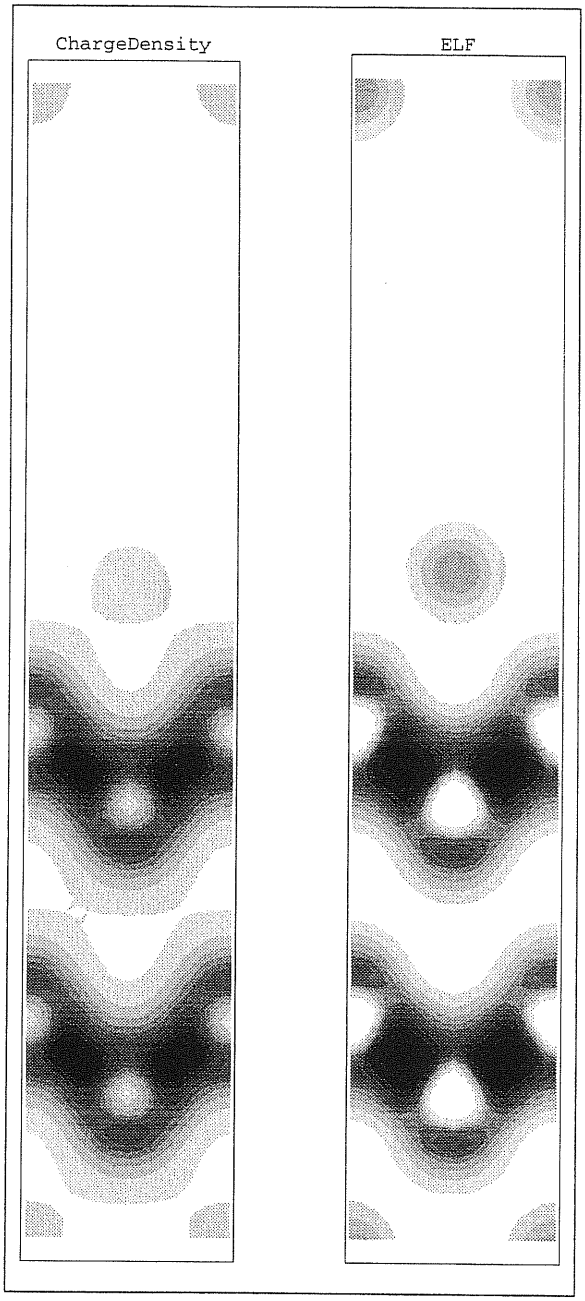

Figure 2.10: Charge density and ELF for the [001] bulk terminated silicon surface. Plane orthogonal to the dangling bond, passing through the center of the surface unit cell.

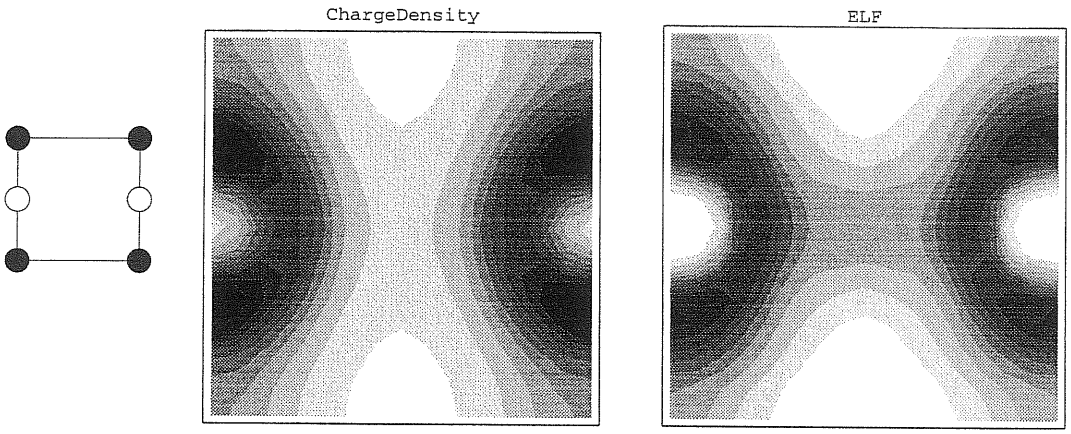

Figure 2.11: Charge density and ELF for the [001] bulk terminated silicon surface. Top view of the surface plane. We report also the schematic surface top view with the same conventions of Fig. (2.7).

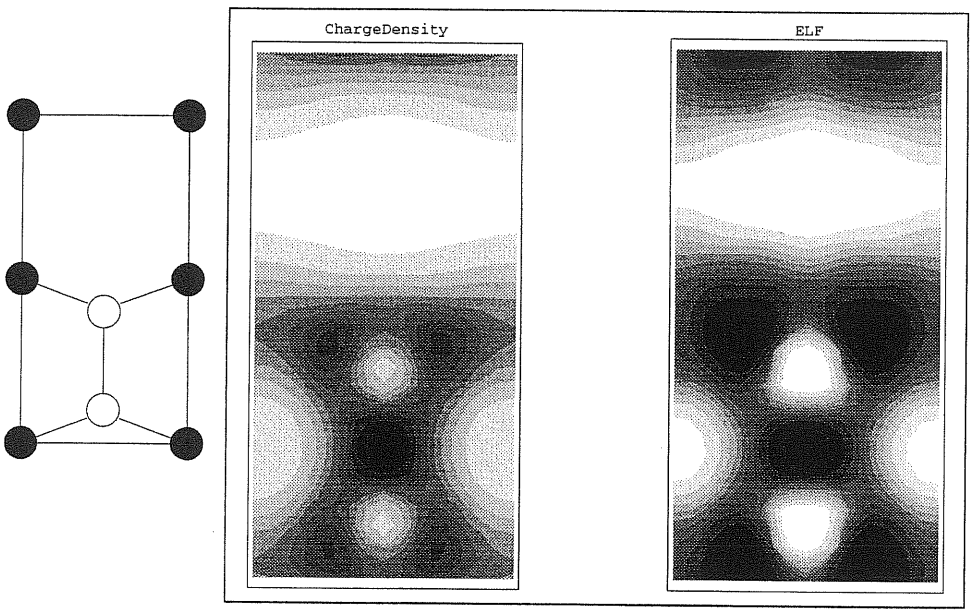

Figure 2.12: Charge density and ELF for the [001] (2×1) symmetric dimer silicon surface. Top view of the surface plane, containing the dimer bond. Conventions as in Fig. (2.11).

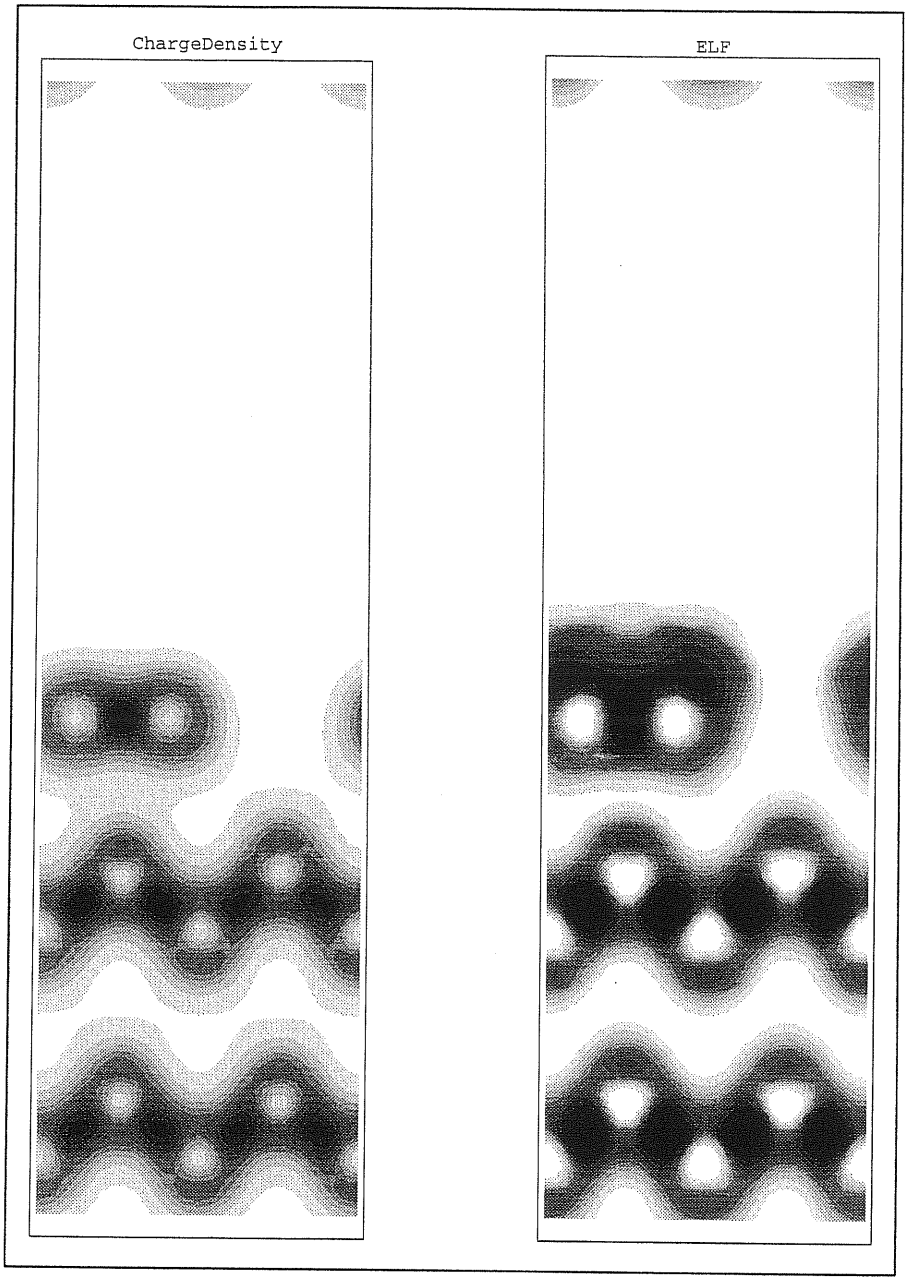

Figure 2.13: Charge density and ELF for the [001] (2×1) symmetric dimer silicon surface. Plane of the dimer bond.

Bibliography

[1] P. Hohenberg and W. Kohn, Phys. Rev **136** B864 (1964).

[2] L.H. Thomas, Proc. Camb. Phil. Soc. **23**, 542 (1927); E. Fermi, Z. Phys. **48**, 73 (1928). Reprinted in N. H. March *Self-Consistent Fields in Atoms* (Pergamon, Oxford, 1975).

[3] W. Kohn and L. J. Sham, Phys. Rev. **140**, A1133 (1965).

[4] M. Levy and J. P. Perdew *Density Functional Methods in Physics*, NATO ASI Series B123 (R. M. Dreizler, J. da Providencia Eds), (Plenum, 1985).

[5] J. E. Harriman, Phys. Rev. A **24**, 680 (1981).

[6] A. D. Becke, K. E. Edgecombe, J. Chem. Phys **92**, 5397 (1990).

[7] A. Savin, O. Jepsen, J. Flad, O. K. Andersen, H. Preuss and H. G. von Schneiring, Angew. Chem. Int. Ed. Engl. **31**, 187 (1992).

[8] G. Zumbach. K. Maschke, Phys. Rev. A **28**, 544 (1983).

[9] F. Gygi, Phys. Rev. B **48**, 11692 (1993).

[10] J. E. Harriman, *Density Matrices and Density Functionals* (R. Erdahl, V. H. Smith Eds), (Reidel, 1987).

[11] R. F. W. Bader and H. Essen, J. Chem. Phys **80**, 1943 (1984).

[12] R. P. Sagar, A. C. T. Ku, V. H. Smith, Jr. and A. Simas, J. Chem. Phys **88**, 4367 (1988).

[13] D. R. Hamman, M. Schlüter and C. Chiang, Phys. Rev. Lett. **43**, 1494 (1979); W. E. Pickett, Comput. Phys. Rep. **9**, 115 (1989).

[14] M. Kohout and A. Savin, J. Comp. Chem. **18**, 1431 (1997).

[15] J. C. Phillips, Rev. Mod. Phys. **42**, 317 (1970); *Bonds and Bands in Semiconductors*, (Academic, New York, 1973).

[16] M. Kohout, A. Savin, J. Flad, H. Preuss and H. G. von Schneiring *Computer Aided Innovation of New Materials II* (M. Doyama, J. Kihara, M. Tanaka, R. Yamamoto Eds), (Elsevier, 1993).

[17] J.D. Jackson, *Classical Electrodynamics* (Wiley, New York, 1975).

[18] A. Baldereschi, S. Baroni, and R. Resta, Phys. Rev. Lett **61**, 734 (1988).

[19] N. Roberts and R. J. Needs, Surf. Sci. **236**, 112 (1990).

[20] H. J. Monkhorst and J. D. Pack, Phys. Rev. B **13**, 5188 (1976).